JACS Au
AN OPEN ACCESS JOURNAL OF THE AMERICAN CHEMICAL SOCIETY

Open Access
This article is licensed under CC-BY-NC-ND 4.0

pubs.acs.org/jacsau
Article

Photochemical Synthesis of β-N-Heterocycle Alcohols via a Coordination-Induced 1,5-Boronate Sigmatropic Rearrangement

Peng Zou,[#] Dongmin Fu,[#] Jihao Jin,[#] Chenyang Xu,[#] Ruijing Cai, Shi-Jun Li, Yi Zeng,* Yu Lan,* and Yiyun Chen*

Cite This: JACS Au 2026, 6, 4458−4468
Read Online
ACCESS | Metrics & More | Article Recommendations | Supporting Information

ABSTRACT: Excited-State Intramolecular Proton Transfer (ESIPT) is an ultrafast nonradiative relaxation pathway that frequently dominates the photophysical fate of conjugated enols, often precluding productive photochemical transformations. Here, we report that bidentate boronate coordination effectively suppresses this process, locking β-N-heterocycle enols into a rigid configuration to enable an efficient photochemical synthesis of β-N-heterocycle alcohols via a 1,5-boronate sigmatropic rearrangement. This strategy circumvents the inherent challenges of hydroxyl acidity and low π-electrophilicity characteristic of the ground-state enol manifold. Operating under mild, metal- and base-free conditions, this protocol facilitates the assembly of 61 diverse aromatic and nonaromatic β-N-heterocycle alcohols (up to 81% yield) using sp^3-, sp^2-, and *sp*-hybridized organoboronic acids. The methodology exhibits high chemo- and regioselectivity—uniquely favoring 1,5-migration to the enol α-carbon over 1,3-addition to the imine—and is well-suited for the late-stage functionalization of complex pharmaceuticals. Comprehensive mechanistic studies, integrating picosecond transient absorption (TA) spectroscopy with DFT modeling, identify a discrete excited-state triplet enol as the pivotal intermediate. Crucially, our findings demonstrate that these boronate−enol photochemical transformations proceed via concerted sigmatropic pathways rather than previously assumed photoactivated nucleophilic additions. This work establishes a robust platform for exploiting coordination-induced kinetic control to modulate photochemical outcomes in enol-based substrates.

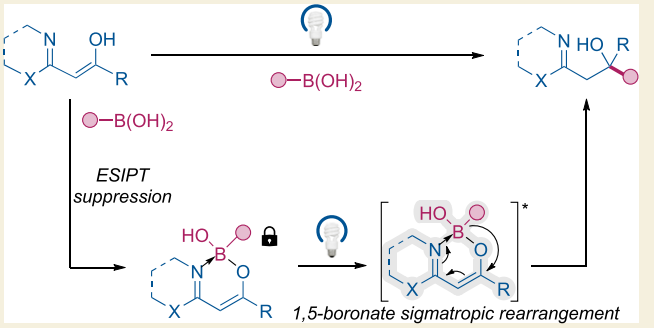

KEYWORDS: *photochemistry, sigmatropic rearrangement, N-heterocycles, excited-state intramolecular proton transfer, boronate complexes*

INTRODUCTION

β-N-Heterocyclic ketones are ubiquitous motifs in medicinal chemistry, serving as essential precursors to bioactive molecules that features β-N-heterocycle tertiary alcohol moieties, including the antifungal agent Quilseconazole and various interleukin-1 receptor antagonists (Figure 1A).[1] However, the direct synthesis of these β-N-heterocycle alcohols from their parent ketones faces a significant reactivity constraints rooted in the thermodynamic stability of their enol tautomers.[2] The inherent acidity of the enol hydroxyl group, combined with the remarkably low π-electrophilicity of the conjugated system, generally precludes direct nucleophilic addition at the enol α-carbon. Consequently, these enols are often biased toward β-carbon functionalization, yielding substituted ketones rather than the high-value β-N-heterocycle alcohol targets.[3]

Traditional strategies to overcome this bias involve the use of Lewis acids to stabilize the ketone moiety,[4] or the employment of potent organometallic nucleophiles (e.g., Grignard or organolithium reagents) to trap transient ketone species (Figure 1B).[5] However, such approaches frequently necessitate cryogenic temperatures and often exhibit restricted functional group tolerance due to the inherently harsh reaction conditions. While organoboronic acids are versatile alternatives for C−C bond formation,[6] their application to β-N-heterocyclic enols remains relatively limited. Previous efforts in photochemical boronate rearrangement to ketones or imines have expanded the scope of these transformations;[7] yet, they have largely been categorized as photoactivated nucleophilic additions—a classification that may not fully account for the reactivity of the predominant enol tautomer, which lacks traditional electrophilic character.[8]

We hypothesized that the latent reactivity of these enols could be assessed by managing their photophysical relaxation. Specifically, we questioned whether boronate coordination could be leveraged to suppress Excited-State Intramolecular Proton Transfer (ESIPT) of enols—the ultrafast (femtosecond

Received: March 25, 2026
Revised: May 26, 2026
Accepted: May 27, 2026
Published: June 11, 2026



© 2026 The Authors. Published by American Chemical Society

Downloaded from pubs.acs.org/jacsau/article-pdf/6/8/4458/6626357/jacsau.6c00455.pdf by SHANGHAI INST OF ORGANIC CHEMISTRY, Yiyun Chen on 07 September 2026

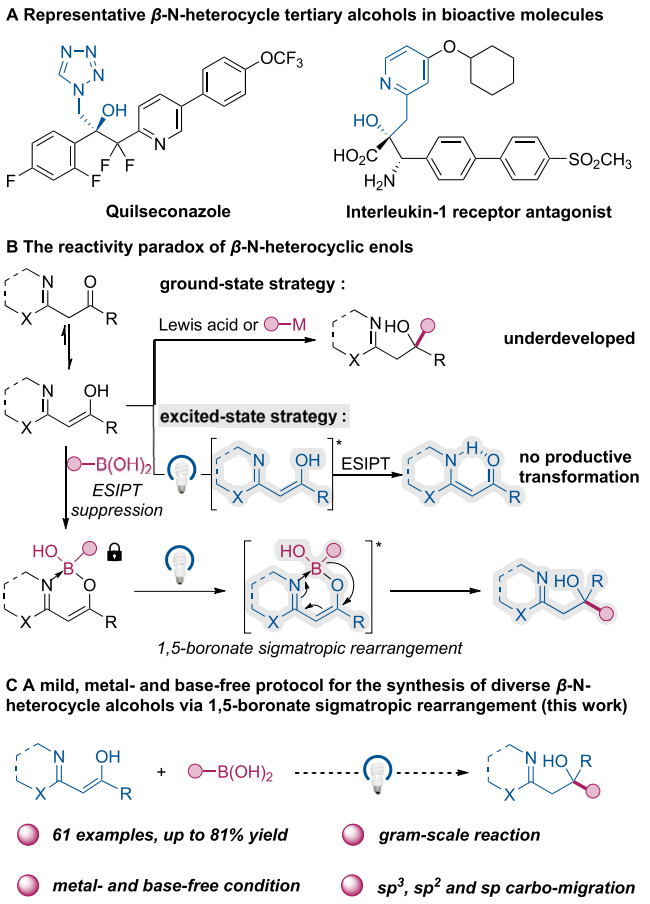

Figure 1. Conceptual framework and discovery of the 1,5-boronate sigmatropic rearrangement. (A) Representative β-N-heterocycle alcohols in bioactive molecules. (B) The reactivity paradox of β-N-heterocyclic enols: High hydroxyl acidity and low π-electrophilicity in the ground state, and Excited-State Intramolecular Proton Transfer (ESIPT) in the excited state. Strategic design: Boronate coordination effectively suppresses ESIPT, locking the reactive enol tautomer to enable the photochemical 1,5-sigmatropic rearrangement. (C) Our work: A mild, metal- and base-free protocol for the synthesis of diverse β-N-heterocycle alcohols via 1,5-boronate sigmatropic rearrangement featuring sp^3, sp^2 and sp carbo-migration (61 examples).

to picosecond) nonradiative process that typically dominates the photophysical fate of conjugated enols (*vide infra*).[9] By implementing bidentate coordination to the N-heterocycle, we envisioned locking the β-N-heterocycle enol substrate into a rigid enol configuration, thereby bypassing ESIPT and redirecting the excited-state energy toward a concerted 1,5-boronate sigmatropic rearrangement (Figure 1B).[10]

Herein, we report the visible-light-driven 1,5-boronate sigmatropic rearrangement of β-N-heterocycle enols. Operating under mild, metal- and base-free conditions, this protocol provides a direct, sigmatropic route to over 60 diverse β-N-heterocycle alcohols (Figure 1C). Beyond its broad synthetic utility, this work couples picosecond transient absorption (TA) spectroscopy with DFT calculations to elucidate the underlying mechanism of boronate−enol photochemistry. Crucially, we demonstrate that these transformations proceed via a discrete excited-state triplet concerted pathway, offering a distinct alternative to classical paradigms of organoboronate reactivity.

RESULTS AND DISCUSSION

Discovery of Photochemical 1,5-Boronate Rearrangement

We previously described a 1,3-boronate rearrangement directed by *o*-hydroxy acetophenone imines, wherein the phenolic hydroxyl group facilitates boronate chelation and subsequent migration to the ketimine center (Table 1A).[7b]

Table 1. Discovery and Regioselectivity of the Photochemical 1,5-Boronate Rearrangement[a]

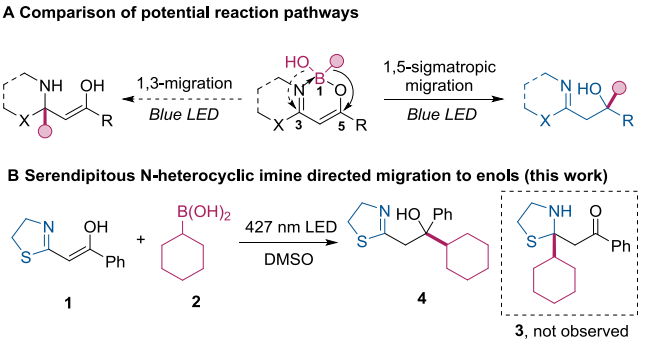

Entry	Conditions	Yield of 4
1	10 W 427 nm, DMSO	(60%)
2	*w/o* light	n.p.
3	80°C	n.p.

[a](A) Comparison of potential reaction pathways: The anticipated 1,3-migration to the electrophilic imine carbon (not observed) versus the discovered 1,5-sigmatropic migration to the enol α-carbon. (B) Model reaction between thiazolinyl enol **1** and cyclohexylboronic acid **2**, demonstrating the exclusive formation of β-thiazolinyl alcohol **4**. Reaction conditions: N-heterocycle enol (0.10 mmol) and boronic acid (0.20 mmol) in anhydrous DMSO (2.0 mL) under 10 W 427 nm LED irradiation at room temperature for 12 h under N_2 atmosphere. Isolated yields are provided. See Supporting Information Table S2−S8 for detailed optimization and control experiments.

Given the structural parallels between *o*-hydroxy imines and β-N-heterocyclic enols, we questioned whether an enol system could similarly direct a boronate rearrangement, potentially mimicking the reactivity patterns observed in 1,3-dicarbonyl systems.[7a] To test this hypothesis, thiazolinyl enol **1** was synthesized as a model substrate. ^{1}H NMR analysis confirmed that **1** exists exclusively as the enol tautomer in solution, with no detectable ketone isomer (see Supporting Information).

Mixing enol **1** with cyclohexyl boronic acid **2** resulted in a distinct bathochromic shift in the UV−vis absorption spectrum, indicating the formation of a rigid boronate-enol complex. This chelation appears to serve a dual function: it lowers the excitation energy into the visible range (427 nm) and significantly restricts the internal degrees of freedom of the substrate. We hypothesized that this restriction would suppress the ultrafast ESIPT typically observed in free enols,[10] effectively locking the molecule in a reactive enol configuration throughout the excited-state manifold.

Subsequent irradiation of the *in situ* mixture with 427 nm blue light afforded the β-thiazolinyl alcohol **4** in 60% isolated yield. Notably, the anticipated 1,3-ketimine addition product **3**—the expected outcome of a conventional photoactivated nucleophilic addition—was not observed. This regiochemical divergence is highly significant; it represents a 1,5-sigmatropic carbo-migration to the enol α-carbon, challenging the

Downloaded from pubs.acs.org/jacsau/article-pdf/6/8/4458/6626357/jacsau.6c00455.pdf by SHANGHAI INST OF ORGANIC CHEMISTRY, Yiyun Chen on 07 September 2026

https://doi.org/10.1021/jacsau.6c00455
JACS Au 2026, 6, 4458−4468

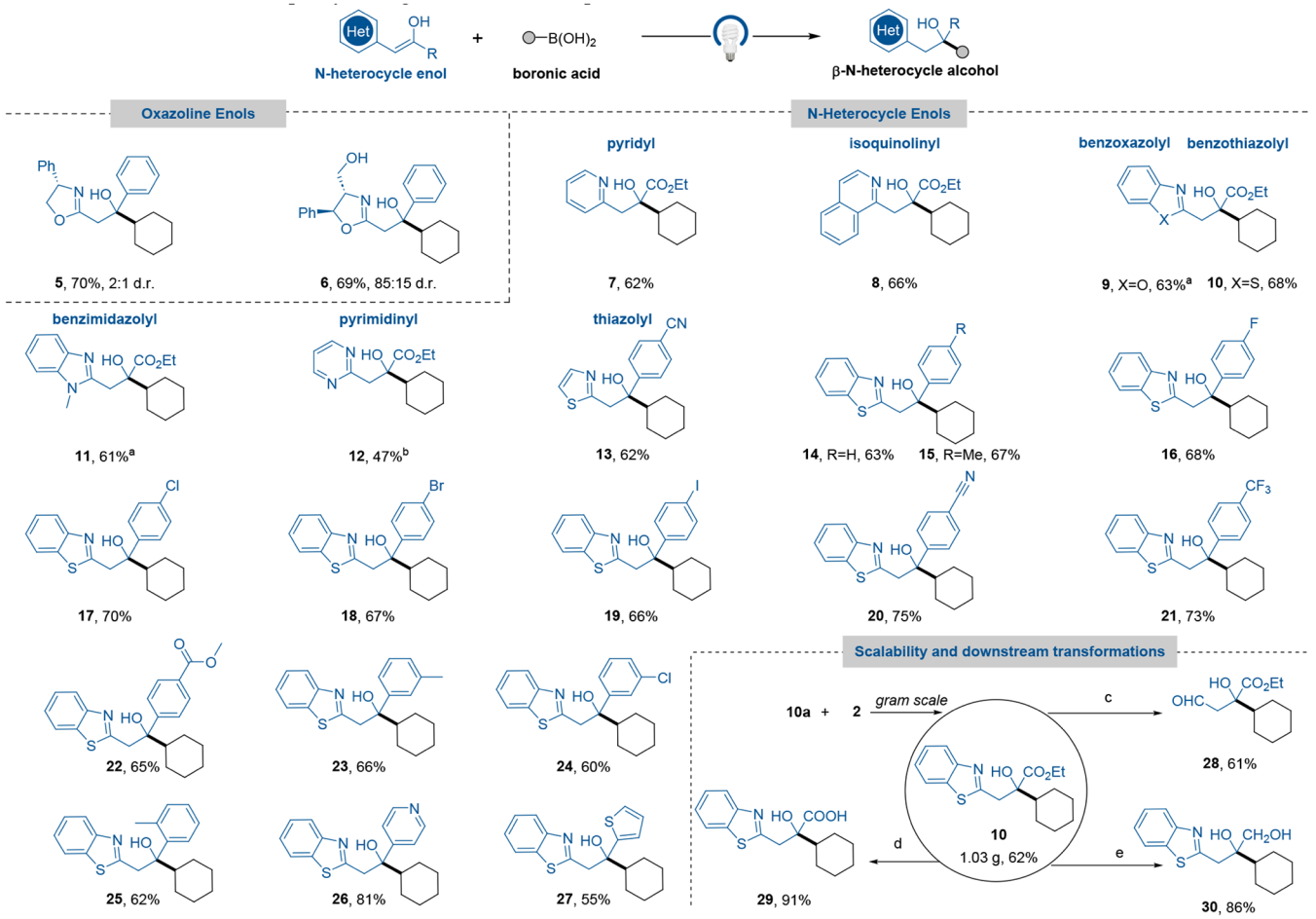

Figure 2. Scope of N-heterocycle enols and synthetic utility. (A) Expansion to oxazoline enols and stereochemical probes. (B) Evaluation of diverse N-heterocyclic scaffolds including pyridyl, isoquinolinyl, and five-membered benzofused systems. (C) Functional group tolerance showcasing the compatibility of the metal-free rearrangement with sensitive electrophiles (nitriles, esters, halides). (D) Gram-scale synthesis and downstream diversification of *β*-N-heterocycle alcohols into high-value synthetic intermediates. Reaction conditions: N-heterocycle enol (1.0 equiv) and boronic acid (2.0 equiv) in anhydrous DMSO (0.05 M) under 10 W 427 nm LED irradiation at room temperature for 12 h under N_2 atmosphere. All yields refer to isolated products after chromatographic purification. [a]DCM was used as the solvent. [b]20 W 427 nm. Sequence for the transformation of the benzothiazole moiety to an aldehyde: [c]MeI then $NaBH_4$ then hydrolysis. [d]LiOH. [e]$LiAlH_4$.

conventional assumption that such migrations are restricted to the traditionally electrophilic imine site under ground-state conditions. Optimization studies revealed that DMSO provided the optimal environment for this transformation in the absence of any additive. Control experiments confirmed the absolute necessity of light, as thermal activation (80 °C) resulted in no conversion, further supporting a photochemical rather than a ground-state pathway (Table 1B).[11]

Expansion to Oxazoline Enols and Stereochemical Probes

To further evaluate the generality of the 1,5-migration, we prepared oxazoline enols **5a**–**6a** as alternative N-heterocyclic scaffolds. Upon complexation with cyclohexyl boronic acid **2**, these substrates underwent efficient 1,5-alkyl migration to afford alcohols **5**–**6** in 69–70% yields. Notably, significant remote diastereoselectivity was observed (**5**, 2:1 d.r.; **6**, 85:15 d.r.). This degree of stereocontrol across a 1,5-system—where the inducing stereocenter and the forming C–C bond is separated by multiple atoms—provides preliminary evidence for a concerted, intramolecular pathway. Such stereochemical integrity is inconsistent with a stepwise radical dissociation–recombination mechanism, which would typically involve loss of diastereomeric purity through the formation of planar or rapidly inverting radical intermediates.

Broad Applicability across N-Heterocycle Enols

To evaluate the generality of the 1,5-boronate sigmatropic rearrangement, we investigated a structurally diverse library of *β*-substituted aromatic N-heterocycle enols (Figure 2). Substrates bearing pyridyl (**7a**), isoquinolinyl (**8a**), benzoxazolyl (**9a**), benzothiazolyl (**10a**), benzimidazolyl (**11a**), pyrimidinyl (**12a**) and thiazolyl (**13a**)—all common pharmacophores—underwent efficient *in situ* boronate formation followed by smooth rearrangement to afford *β*-N-heterocycle alcohols (**7**–**13**) in 47–68% yields.

A defining feature of this photochemical protocol is its exceptional chemoselectivity. The reaction tolerated a wide array of sensitive functional groups, including aryl halides, nitriles, trifluoromethyl groups, and esters, providing the corresponding products (**14**–**25**) in 60–75% yields. Notably, preservation of electrophilic nitriles and esters under these conditions highlights a significant advantage over traditional organometallic strategies. While conventional organometallic nucleophiles (e.g. organolithium or Grignard reagents) trigger unavoidable side reactions at these electrophilic centers even

https://doi.org/10.1021/jacsau.6c00455
JACS Au 2026, 6, 4458–4468

Downloaded from pubs.acs.org/jacsau/article-pdf/6/8/4458/6626357/jacsau.6c00455.pdf by SHANGHAI INST OF ORGANIC CHEMISTRY, Yiyun Chen on 07 September 2026

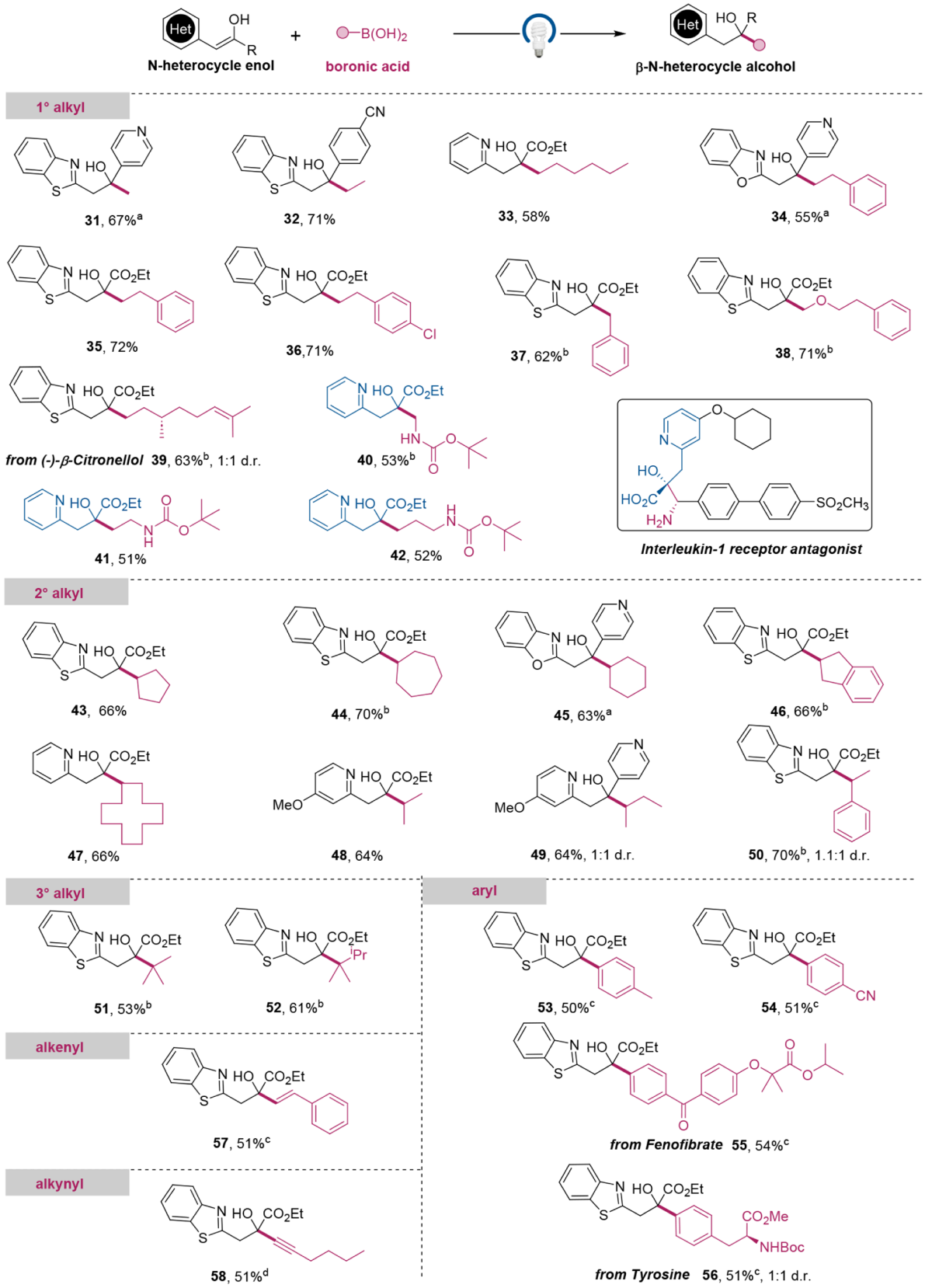

Figure 3. Versatility of boronic acids in the 1,5-sigmatropic rearrangement. Substrate scope evaluation across sp^3, sp^2, and sp-hybridization states. (A) Primary and secondary alkyl boronic acids, including terpenoid and amino acid derivatives (**39**, **40**−**42**). (B) Sterically demanding secondary and tertiary alkyl boronic acids, featuring the construction of adjacent quaternary centers (**51**, **52**). (C) Aryl and alkenyl boronic acids, including late-stage functionalization of the cholesterol-reducing drug fenofibrate (**55**) and a tyrosine derivative (**56**). (D) Rare 1,5-alkynyl migration yielding tertiary propargyl alcohol (**58**). Reaction conditions: N-heterocycle enol (1.0 equiv) and boronic acid (2.0 equiv) in anhydrous DMSO (0.05 M) under 10 W 427 nm LED irradiation at room temperature for 12 h under N_2 atmosphere. All yields are for isolated products after chromatographic

https://doi.org/10.1021/jacsau.6c00455
JACS Au 2026, 6, 4458−4468

Downloaded from pubs.acs.org/jacsau/article-pdf/6/8/4458/6626357/jacsau.6c00455.pdf by SHANGHAI INST OF ORGANIC CHEMISTRY, Yiyun Chen on 07 September 2026

Figure 3. continued

purification. [a]3.0 equiv. boronic acid. [b]Potassium organotrifluoroborate used in DCM/H_2O. [c]DCM as solvent, 20 W 427 nm LED, 18 h. [d]3.0 equiv. organotrifluoroborate in DCM/H_2O, 20 W 427 nm LED, 18 h.

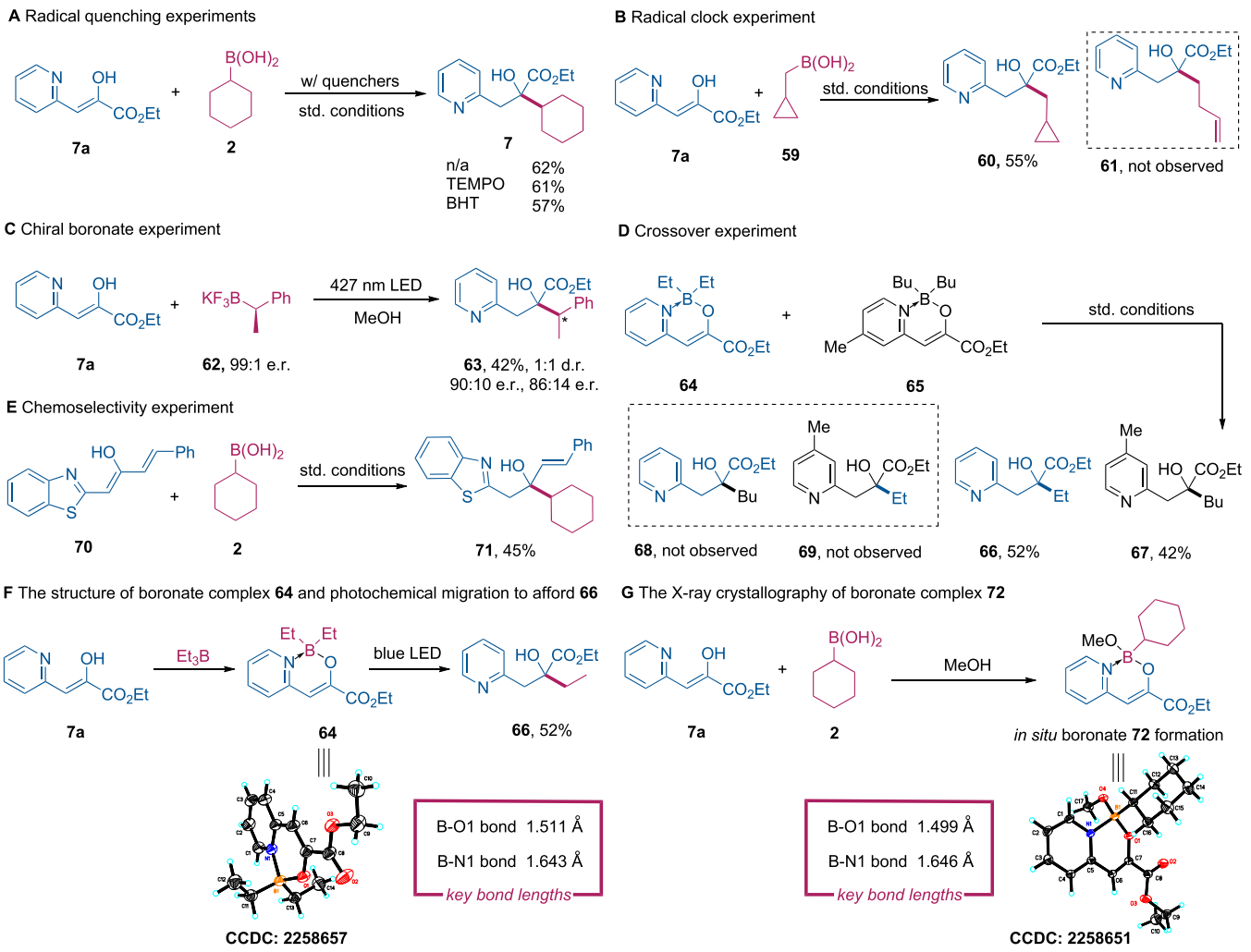

Figure 4. Mechanistic investigations and structural characterization. (A) Radical quenching experiments with TEMPO and BHT confirming the absence of a free-radical chain pathway. (B) Radical clock experiment using cyclopropylmethylboronic acid (**59**); the exclusive formation of unrearranged product **60** excludes long-lived radical intermediates. (C) Stereochemical probe utilizing enantiopure organoboronate **62**, demonstrating significant retention of stereochemical integrity in adduct **63**, consistent with a concerted intramolecular migration. (D) Crossover experiment between boronates **64** and **65** confirming the strictly intramolecular nature of the 1,5-rearrangement. (E) Regioselectivity probe with alkenyl enol **70** demonstrating exclusive 1,5-migration over 1,7-addition. (F) X-ray crystal structure of triethylborane-derived complex **64** (ORTEP diagram at 50% probability; hydrogen atoms and ethyl groups omitted for clarity), revealing a tetracoordinate boron center (THC = 0.83). (G) X-ray crystal structure of cyclohexylboronic acid-derived complex **72** (THC = 0.87).

under cryogenic temperatures, this metal- and base-free approach proceeds with high fidelity at room temperature. Furthermore, pyridyl- and thiophenyl-substituted enols (**26a**–**27a**) participated effectively (55–81% yields), demonstrating that additional Lewis-basic sites do not interfere with the critical bidentate boronate chelation required for the 1,5-migration.

Scalability and Downstream Transformations

The synthetic robustness of the 1,5-boronate rearrangement was further demonstrated through a gram-scale synthesis. The reaction of **10a** and **2** was scaled to 5.0 mmol, providing β-benzothiazolyl alcohol **10** in 62% yield (1.03 g) without a loss in efficiency. The resulting β-N-heterocycle alcohols serve as versatile synthetic handles. For example, the benzothiazole moiety in **10** was converted into aldehyde **28** in a one-pot sequence (61% yield), offering a streamlined route to functionalized β-hydroxy aldehydes.[12] Additionally, **10** was smoothly hydrolyzed to lactate **29** (91% yield) or reduced to 1,2-diol **30** (86% yield). These transformations underscore the utility of the N-heterocycle as a "masked" functional group, allowing for the rapid assembly of complex 1,3-difunctionalized motifs.

Broad Compatibility with sp^3, sp^2, and sp carbo-Groups

The versatility of the 1,5-boronate sigmatropic rearrangement was further evaluated across a diverse range of organoboronic acids (Figure 3). Primary alkyl boronic acids, including methyl,

https://doi.org/10.1021/jacsau.6c00455
JACS Au 2026, 6, 4458–4468

Downloaded from pubs.acs.org/jacsau/article-pdf/6/8/4458/6626357/jacsau.6c00455.pdf by SHANGHAI INST OF ORGANIC CHEMISTRY, Yiyun Chen on 07 September 2026

ethyl, and long-chain aliphatic and benzyl derivatives (**31b**–**38b**), underwent efficient photochemical 1,5-migration to yield the corresponding β-N-heterocycle alcohols (**31**–**38**) in 55–71% yields.[13] The reaction demonstrated exceptional tolerance for steric bulk: secondary cyclic alkyl boronates (five- to 12-membered rings, **43b**–**47b**) and acyclic variants (**48b**–**50b**) consistently afforded products in 63–70% yields. Most notably, the protocol accommodated sterically congested tertiary alkyl boronic acids; the *tert*-butyl-substituted product **51** (53%) and the highly hindered **52** (61%) were successfully synthesized, even when generating two adjacent quaternary carbon centers.

The utility of this method extends to sp^2-hybridized aryl and alkenyl boronates (**53b**–**54b**, **57b**), yielding benzyl and tertiary allyl alcohols with high efficiency. Highlighting the unique mechanistic capabilities of this 1,5-migration, an alkynyl boronic acid (**58b**) successfully participated to afford the tertiary propargyl alcohol **58** (51%). Such 1,5-alkynyl migrations are infrequently observed in photochemical systems and underscore the broad applicability of the sigmatropic pathway, which extends significantly beyond the scope of traditional ground-state rearrangements or our previously reported photochemical additions.[7,14]

Late-Stage Functionalization (LSF) of Bioactive Molecules

To evaluate the potential of this metal- and base-free transformation in a medicinal chemistry context, we applied the protocol to the late-stage functionalization of complex, drug-like scaffolds. A (−)-β-citronellol-derived boronate was incorporated to furnish terpenoid-conjugated molecule **39** (63% yield). Furthermore, amino boronic acids (**40b**–**42b**) provided efficient access to β-, γ-, or δ-pyridyl-substituted amino alcohols (**40**–**42**), motifs found in interleukin-1 receptor antagonists.[15] The robustness of the reaction was further evidenced by the successful incorporation of a fenofibrate-derived boronic acid (a hypolipidemic drug) and a tyrosine-derived boronic acid, yielding the drug-conjugates **55** (54%) and **56** (51%), respectively.[16] The absence of aggressive reagents or heavy metals makes this methodology a promising candidate for the diversification of complex, sensitive pharmaceuticals where structural integrity is paramount.

Mechanistic Investigations

To elucidate the nature of the C–C bond-forming step, we conducted a series of experimental probes designed to distinguish between radical-chain, dissociative, and concerted sigmatropic pathways (Figure 4). First, the involvement of free-radical intermediates was scrutinized (Figure 4A–C).[17] The 1,5-rearrangement of **7a** proceeded with high efficiency in the presence of radical scavengers such as TEMPO (61% yield) and BHT (57% yield), indicating that a free-radical chain mechanism is unlikely (Figure 4A).[18] This conclusion was corroborated by a measured quantum yield of 0.62; a value below unity suggests a radical chain propagation process unlikely (see Supporting Information). To probe for the generation of short-lived radical species, we employed cyclopropylmethylboronic acid (**59**) as a radical clock precursor. The reaction yielded exclusively the unrearranged product **60** (55%), with no detectable ring-opened product **61** (Figure 4B).[19] Given the rapid rate of cyclopropylmethyl radical rearrangement, the exclusive formation of **60** strongly suggests the absence of any transient radical intermediates with a significant lifetime.

Crucially, when enantiopure organoboronate **62** (99:1 e.r.) was reacted with **7a**, the resulting adduct **63** exhibited significant retention of stereochemical integrity (90:10 and 86:14 e.r. for the respective diastereomers, Figure 4C) (see Supporting Information for more examples).[20] This high degree of enantiospecificity, coupled with the absence of radical signals in nanosecond electron paramagnetic resonance (EPR) spectroscopy (Figure S15), strongly supports a concerted, intramolecular migration occurring within a tight solvent cage or via a sigmatropic transition state.

To confirm the intramolecular nature of the carbo-migration, a crossover experiment was performed using two boronates, **64** and **65**, possessing different alkyl groups and N-heterocycle scaffolds. Under standard conditions, only the intramolecular rearrangement products **66** and **67** were observed; no intermolecular crossover products (**68** or **69**) were detected by HRMS analysis of the crude reaction mixture (Figure 4D).

The inherent regioselectivity of the excited-state process was further highlighted using the conjugated alkenyl enol **70**. The reaction yielded the 1,5-migration product **71** (45%) exclusively (Figure 4E). The absence of 1,7-conjugate addition products—typical outcomes in radical-mediated additions to extended π-systems[21]—further reinforces the classification of this transformation as a sigmatropic rearrangement. These results collectively demonstrate that the in situ-generated boronate complex undergoes a highly ordered, intramolecular 1,5-migration steered by the electronic configuration of the excited-state enol.

X-ray Crystallographic Analysis of N-Heterocycle Enol-Boronate Chelates

To definitively characterize the reactive species, β-pyridyl enol ester **7a** was reacted with triethylborane, resulting in the spontaneous evolution of ethane and the formation of boronate complex **64** (Figure 4F). X-ray crystallographic analysis revealed a tetracoordinate boron center with 83% tetrahedral character (THC = 0.83), as determined by Höpfl's equation.[22] Crucially, the crystal structure confirms that the pyridyl enol ester is "locked" in its enol form upon chelation, forming a robust bidentate complex with a covalent B–O bond (1.511 Å) and a dative B ← N bond (1.643 Å).[23] Subsequent irradiation of the isolated complex **64** with blue LEDs afforded the β-pyridyl alcohol **66** in 52% yield, confirming that this chelate is a competent intermediate in the rearrangement.

To mirror the *in situ* reaction conditions, the interaction between **7a** and cyclohexyl boronic acid **2** was investigated. Mixing the two components resulted in the emergence of a characteristic tetracoordinate signal at 8.39 ppm in the ^{11}B NMR spectrum, accompanied by a concomitant decrease in the intensity of the free boronic acid peak (Figures S2–S3). High-resolution mass spectrometry confirmed the dehydration-driven formation of the boronate (Figure S4). Single crystals of the resulting complex **72** were obtained from methanol and analyzed via X-ray diffraction (Figure 4G). Complex **72** displayed a similarly high tetrahedral character (THC = 0.87) and bond lengths (B–O: 1.499 Å; B ← N: 1.646 Å) consistent with those of complex **64**. The thermodynamic stability of this *in situ* assembly was quantified using Benesi–Hildebrand analysis, which revealed a strong binding association constant (K_a) of 54.5 M^{-1} (Figures S5–S6).[24] This robust association constant explains the protocol's efficiency in the absence of exogenous metals or bases; the self-assembly of the boronate-

Downloaded from pubs.acs.org/jacsau/article-pdf/6/8/4458/6626357/jacsau.6c00455.pdf by SHANGHAI INST OF ORGANIC CHEMISTRY, Yiyun Chen on 07 September 2026

https://doi.org/10.1021/jacsau.6c00455
JACS Au 2026, 6, 4458–4468

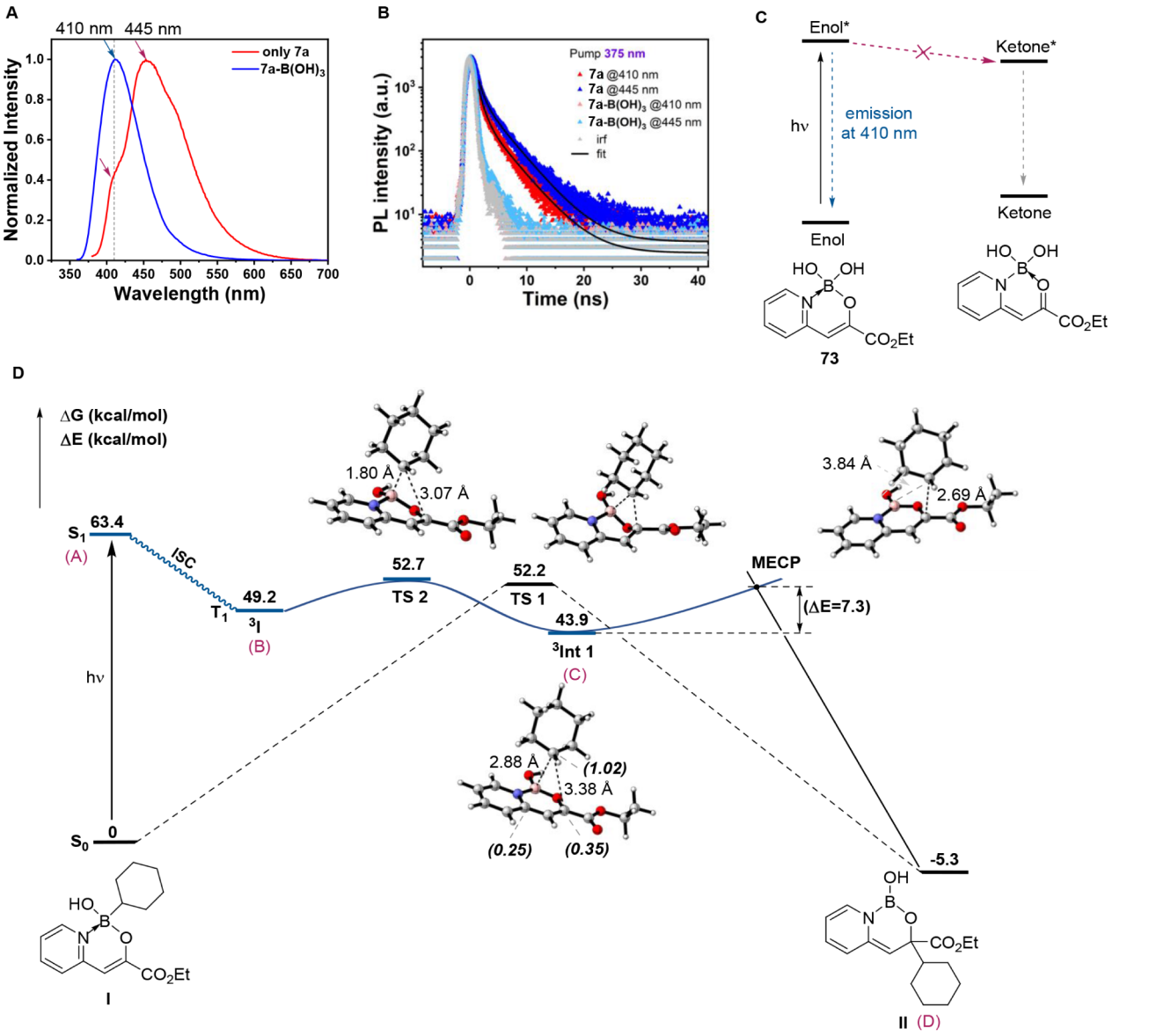

Figure 5. Photophysical and computational investigations of the sigmatropic rearrangement pathway. (A) Normalized fluorescence spectra of free N-heterocycle enol **7a** (red) and boronate complex **73** (blue) excited at 340 nm. The single emission peak of **73** vs the dual emission of **7a** indicates the suppression of Excited-State Intramolecular Proton Transfer (ESIPT). (B) Time-resolved photoluminescence (PL) of **7a** and **73** monitored at 410 and 445 nm (pulse excitation at 375 nm). The monoexponential decay of **73** (0.4 ns) confirms the "locking" of the enol tautomer. (C) Calculated Gibbs free energy profile (M06−2X/6−31G*) for the 1,5-boronate sigmatropic rearrangement. (D) Optimized geometries of key transition states (**TS1**, **TS2**) and the spin-separated triplet intermediate (^{3}**Int 1**), highlighting the concerted but nonsynchronous nature of the C−B bond cleavage and C−C bond formation.

enol chelate is sufficiently favorable to drive the reaction forward under mild, visible-light conditions. These structural data provide a clear physical basis for our proposed mechanism, demonstrating that the boronate moiety organizes the enol into a rigid, photoactive geometry optimized for 1,5-migration.

Spectroscopic Evidence for ESIPT Suppression

To elucidate the photophysical consequences of boronate coordination, we conducted extensive spectroscopic investigations to distinguish our findings from established keto-addition pathways (Figure 5A−B). The fluorescence spectrum of free N-heterocycle enol **7a** exhibits dual emission peaks at 410 and 445 nm, a hallmark of Excited-State Intramolecular Proton Transfer (ESIPT) wherein the enol and its ketone tautomer coexist in the excited state.[25] Remarkably, upon boronate complexation, the resulting complex **73** displays a single enol emission peak at 410 nm. This observation indicates that the rigid bidentate coordination effectively locks the substrate, suppressing the ultrafast photoisomerization to the ketone form.[26]

Time-resolved photoluminescence (PL) spectroscopy further confirms this suppression. While the emission decay of free enol **7a** is biexponential—featuring a long-lived ketone component (4.0 ns)—boronate complex **73** exhibits a monoexponential decay with a significantly shorter lifetime (0.4 ns). This shift unequivocally confirms the circumvention of the ESIPT pathway (Figure 5B). These data demonstrate that the reaction proceeds through a mechanism distinct from previously reported photochemical boronate rearrangements,

https://doi.org/10.1021/jacsau.6c00455
JACS Au 2026, 6, 4458−4468

Downloaded from pubs.acs.org/jaucr/article-pdf/6/8/4458/6626385/jacsau.6c00455.pdf by SHANGHAI INST OF ORGANIC CHEMISTRY, Yiyun Chen on 07 September 2026

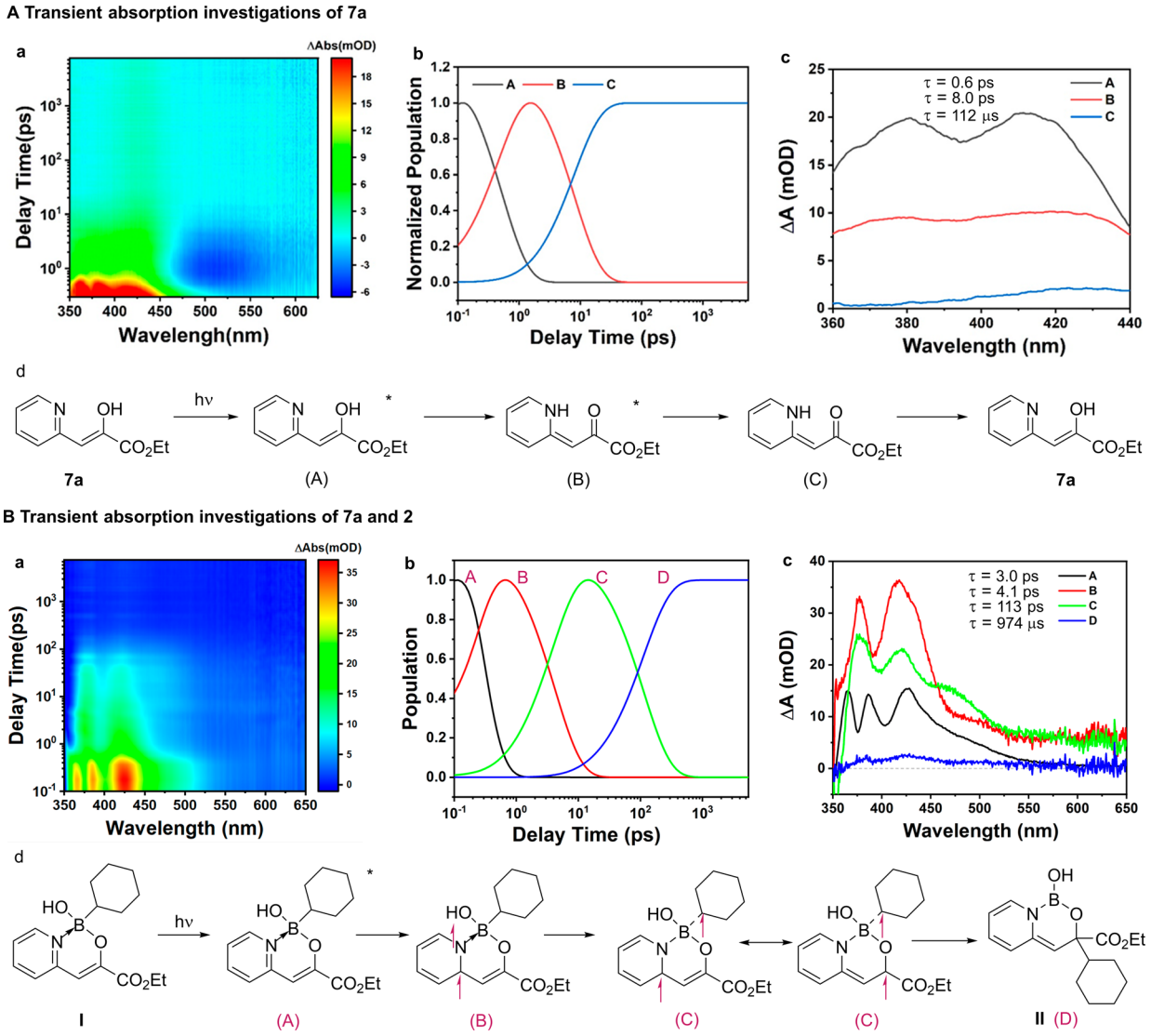

Figure 6. Transient absorption spectroscopy investigations for the photochemical femtosecond intermediates. (A) Transient absorption (TA) investigations of N-heterocycle enol **7a**. a. 2D pseudocolor TA spectra of N-heterocycle enol **7a** within 7 ns following excitation at 340 nm. b. Normalized populations of the three species with colors correlating with the evolution-associated spectra. c. Evolution-associated spectra of the three species fitted by global target analysis using a sequential kinetic model. d. The diagram of the N-heterocycle enol **7a** decay pathway upon excitation. (B) Transient absorption (TA) investigations of N-heterocycle enol **7a** and boronic acid **2**. a. 2D pseudocolor TA spectra of N-heterocycle enol **7a** and boronic acid **2** within 7 ns following excitation at 340 nm. b. Normalized populations of the four species with colors correlating with the evolution-associated spectra. c. Evolution-associated spectra of the four species fitted by global target analysis using a sequential kinetic model. d. The diagram of the boronate complex **I** reaction pathway upon excitation.

which relied on the inherent electrophilicity of the transient ketone tautomer (Figure 5C).[23,27]

Computational Analysis of the 1,5-Sigmatropic Pathway

To quantify the observed reactivity and regioselectivity, density functional theory (DFT) calculations were performed at the M06-2*X*/6-31G* level (Figure 5C–D).[28] In the ground state (S_0), the 1,5-boronate rearrangement of complex **I** to alcohol **II** requires a prohibitively high activation energy of 52.2 kcal/mol, rendering the thermal pathway inaccessible.[7a]

Upon photoexcitation, complex **I** reaches the excited singlet state S_1 (63.4 kcal/mol), followed by efficient intersystem crossing to the triplet state **T1** (49.2 kcal/mol). From the T_1 surface, the reaction bypasses the high thermal barriers of the ground state, proceeding via transition state **TS2** with a remarkably low activation energy of only 3.5 kcal/mol to form intermediate ^{3}**Int 1**. In this triplet intermediate, the C–B distance (2.88 Å) remains within the sum of the van der Waals radii, suggesting that the C–B bond is not fully dissociated—a structural feature consistent with our experimental evidence excluding free-radical intermediates.[29]

Spin population analysis of ^{3}**Int 1** reveals a species with significant spin density localized on the migrating carbon (1.02) and the enol C_5 (0.35). This electronic distribution explains the high regioselectivity for 1,5-migration over 1,3-addition to the N-heterocycle C_3 (0.25). The process concludes via a minimal energy crossing point (MECP), located 7.3 kcal/mol above ^{3}**Int 1**, facilitating spin crossover to the singlet ground state. At the MECP, concurrent C–B cleavage and C–C bond formation (2.69 Å) affects the structural recombination, yielding the boronic acid-coordinated alcohol **II**. This concerted but nonsynchronous pathway

Downloaded from pubs.acs.org/jacsau/article-pdf/6/8/4458/6626357/jacsau.6c00455.pdf by SHANGHAI INST OF ORGANIC CHEMISTRY, Yiyun Chen on 07 September 2026

https://doi.org/10.1021/jacsau.6c00455
JACS Au 2026, 6, 4458–4468

represents a shift in the conceptual understanding of boronate-enol interactions.

Transient Absorption Spectroscopy and Mechanistic Analysis

To resolve the ultrafast kinetics of the 1,5-migration and confirm the suppression of ESIPT, we employed femtosecond transient absorption (TA) spectroscopy (Figure 6). Global target analysis was performed using a sequential kinetic model to deconvolute the excited-state absorption (ESA) spectra of the transient intermediates.[30]

We first examined the TA profile of the free N-heterocycle enol **7a** (Figure 6A). The spectrum of **7a** is dominated by significant stimulated emission (SE), a characteristic feature of rapid Excited-State Intramolecular Proton Transfer (ESIPT). This process occurs on the picosecond time scale, converting the enol to its ketone tautomer. The resulting excited ketone then relaxes into a long-lived ground-state *trans*-ketone, characterized by a persistent absorption band at 460 nm (see Figures S13−S14). The dominance of these nonradiative relaxation pathways explains the traditional lack of 1,2-addition reactivity in free enols.

Spectroscopic Evidence for the Sigmatropic Pathway

In sharp contrast, the TA spectrum of the *in situ*-generated boronate complex **I** exhibited only ESA features, with a complete absence of ketone-stimulated emission (Figure 6B, left panel). This provides direct evidence that boronate coordination effectively suppresses ESIPT by locking the substrate into a rigid, reactive enol configuration.

Global analysis of the transient absorption data for the boronate complex identified four distinct transient species (**A**−**D**) using a sequential fitting model (A → B → C → D). These species correlate exceptionally well with the computed intermediates alongour calculated reaction coordinate (Figure 6B, middle panel): 1). Species A (S_1, τ = 3.0 ps): The initially populated excited singlet state, which undergoes rapid intersystem crossing to the triplet manifold. The B ← N dative bond likely facilitates this rapid spin-flip.[31] 2). Species B (T_1, τ = 4.1 ps): A triplet state localized at the C=N bond. 3). Species C (^{3}Int1, τ = 113 ps): The key spin-separated biradical intermediate identified by DFT calculations. Formed from the decay of species B, its electronic distribution concentrates spin density on the migrating carbon and the enol C5 position, pre-organizing the scaffold to undergo the sigmatropic rearrangement over a 113 ps timeline. 4). Species D (Product-like, τ = 974 μs): The product-like state corresponds to the boronic acid-coordinated β-N-heterocycle alcohol. Populated within 113 ps from species C, nanosecond flash photolysis confirms this ground-state species possesses a long microsecond lifespan (τ = 974 μs)..

Proposed Concerted Mechanism

Based on the synchronization between these spectroscopic lifetimes and the DFT-calculated energy barriers, we propose a concerted 1,5-boronate sigmatropic rearrangement. Upon photoexcitation and coordination-induced suppression of the ESIPT pathway, the system reaches the T_1 state. The subsequent formation of the spin-separated intermediate **C** leads to structural recombination via a minimum energy crossing point (MECP). This allows for concerted C−B bond cleavage and concurrent C−C bond formation, circumventing the need for free-radical intermediates. Final tautomerization and hydrolysis yield the β-N-heterocycle alcohol. This close alignment between transient absorption kinetics and computational modeling rationalizes boronate reactivity as a concerted sigmatropic process, offering a distinct framework for modulating excited-state tautomerization to enable non-canonical transformations.[31]

CONCLUSIONS

In summary, we have established a visible-light-driven 1,5-boronate sigmatropic rearrangement that addresses the long-standing reactivity constraints of β-N-heterocyclic enols. By leveraging bidentate coordination to suppress ESIPT, we demonstrate an effective strategy to outcompete ultrafast nonradiative relaxation pathways. This coordination-induced kinetic lock maintains the substrate in a reactive enol configuration throughout the excited-state manifold, enabling a concerted 1,5-carbo migration that is energetically inaccessible under ground-state conditions.

This metal- and base-free protocol exhibits exceptional functional group tolerance and regioselectivity, providing efficient access to a library of 61 diverse β-N-heterocycle alcohols—including high-value bioactive derivatives—in yields up to 81%. Our mechanistic framework, supported by picosecond TA spectroscopy and DFT calculations, identifies a discrete excited triplet enol as the pivotal intermediate. These findings demonstrate that the reaction proceeds through a concerted sigmatropic pathway, rather than a conventional photoactivated nucleophilic addition. This discovery recontextualizes boronate−enol photochemistry, demonstrating that analogous functionalizations of 1,3-dicarbonyl systems should, under appropriate conditions, be viewed through the lens of sigmatropic rearrangements. We anticipate that this ESIPT-locking strategy will serve as a valuable framework for using temporary coordination to modulate photochemical outcomes, offering a robust platform for the development of sophisticated light-driven transformations.

ASSOCIATED CONTENT

Supporting Information

The Supporting Information is available free of charge at https://pubs.acs.org/doi/10.1021/jacsau.6c00455.

Experimental procedures, mechanistic studies, reaction optimization, spectroscopic experiments, computational studies, characterizations, X-ray crystallographic data, and copies of NMR spectra (PDF)

Accession Codes

Deposition Numbers 2258651 and 2258657 contain the supplementary crystallographic data for this paper. These data can be obtained free of charge via the joint Cambridge Crystallographic Data Centre (CCDC) and Fachinformationszentrum Karlsruhe Access Structures service.

AUTHOR INFORMATION

Corresponding Authors

Yiyun Chen − *State Key Laboratory of Chemical Biology, Shanghai Institute of Organic Chemistry, Chinese Academy of Sciences, University of Chinese Academy of Sciences, Shanghai 200032, China; School of Physical Science and Technology, ShanghaiTech University, Shanghai 201210, China; School of Chemistry and Material Sciences, Hangzhou Institute for Advanced Study, University of Chinese Academy of Sciences,*

Downloaded from pubs.acs.org/jacsau/article-pdf/6/8/4458/6626357/jacsau.6c00455.pdf by SHANGHAI INST OF ORGANIC CHEMISTRY, Yiyun Chen on 07 September 2026

https://doi.org/10.1021/jacsau.6c00455
JACS Au 2026, 6, 4458−4468

Hangzhou 310024, China; orcid.org/0000-0003-0916-0994; Email: yiyunchen@sioc.ac.cn

Yu Lan − *College of Chemistry, and Pingyuan Laboratory, Zhengzhou University, Zhengzhou, Henan 450001, China;* Email: lanyu@cqu.edu.cn

Yi Zeng − *Key Laboratory of Photochemical Conversion and Optoelectronic Materials, Technical Institute of Physics and Chemistry, Chinese Academy of Sciences, University of Chinese Academy of Sciences, Beijing 100190, China;* orcid.org/0000-0003-0694-1795; Email: zengyi@mail.ipc.ac.cn

Authors

Peng Zou − *State Key Laboratory of Chemical Biology, Shanghai Institute of Organic Chemistry, Chinese Academy of Sciences, University of Chinese Academy of Sciences, Shanghai 200032, China*

Dongmin Fu − *College of Chemistry, and Pingyuan Laboratory, Zhengzhou University, Zhengzhou, Henan 450001, China*

Jihao Jin − *Key Laboratory of Photochemical Conversion and Optoelectronic Materials, Technical Institute of Physics and Chemistry, Chinese Academy of Sciences, University of Chinese Academy of Sciences, Beijing 100190, China;* orcid.org/0009-0003-0921-972X

Chenyang Xu − *State Key Laboratory of Chemical Biology, Shanghai Institute of Organic Chemistry, Chinese Academy of Sciences, University of Chinese Academy of Sciences, Shanghai 200032, China*

Ruijing Cai − *State Key Laboratory of Chemical Biology, Shanghai Institute of Organic Chemistry, Chinese Academy of Sciences, University of Chinese Academy of Sciences, Shanghai 200032, China; School of Physical Science and Technology, ShanghaiTech University, Shanghai 201210, China*

Shi-Jun Li − *College of Chemistry, and Pingyuan Laboratory, Zhengzhou University, Zhengzhou, Henan 450001, China;* orcid.org/0000-0001-9872-6245

Complete contact information is available at: https://pubs.acs.org/10.1021/jacsau.6c00455

Author Contributions

#P.Z.,D.F., J.J., and C.X. contributed equally to this work.

Notes

The authors declare no competing financial interest.

■ ACKNOWLEDGMENTS

Financial support was provided by the Strategic Priority Research Program of the Chinese Academy of Sciences (XDB1060000), the National Natural Science Foundation of China (grants 22337005, 22277133), the Shanghai Oriental Talent Leadership Program, the Youth Innovation Promotion Association CAS (2023266), Lingang Laboratory Grant No. LGL-2617-01, the Program for Science and Technology Innovation Talents in Universities of Henan Province (No. 20HASTIT004), and the National Supercomputing Center in Zhengzhou.

■ REFERENCES

(1) (a) La Regina, G.; D'Auria, F. D.; Tafi, A.; Piscitelli, F.; Olla, S.; Caporuscio, F.; Nencioni, L.; Cirilli, R.; La Torre, F.; De Melo, N. R.; et al. 1-[(3-Aryloxy-3-aryl)propyl]-1H-imidazoles, New Imidazoles with Potent Activity against Candida albicans and Dermatophytes. Synthesis, Structure−Activity Relationship, and Molecular Modeling Studies. *J. Med. Chem.* **2008**, *51*, 3841−3855. (b) Vitaku, E.; Smith, D. T.; Njardarson, J. T. Analysis of the structural diversity, substitution patterns, and frequency of nitrogen heterocycles among U.S. FDA approved pharmaceuticals. *J. Med. Chem.* **2014**, *57*, 10257−10274.

(2) Henegar, K. E.; Winkler, J. D. A new method for the synthesis of dioxolenones the carboxylation of ketone enolates with anisyl cyanoformate. *Tetrahedron Lett.* **1987**, *28*, 1051−1054.

(3) Lou, Y.; Lin, Z.; Wu, C.; Nong, Z.-S.; Liu, R.; Gong, L.-Z. Enantioselective Synthesis of Chiral 1,4-Enynes via Palladium-Catalyzed Branch-Selective Allylic C−H Alkylation. *ACS Catal* **2024**, *14*, 14855−14862.

(4) Pocker, Y.; Spyridis, G. T. Modulation of Tautomeric Equilibria by Ionic Clusters. Acetylacetone in Solutions of Lithium Perchlorate−Diethyl Ether. *J. Am. Chem. Soc.* **2002**, *124*, 10373−10380.

(5) Yuan, R.; Zhao, D.; Zhang, L.-Y.; Pan, X.; Yang, Y.; Wang, P.; Li, H.-F.; Da, C.-S. Isopropylmagnesium chloride-promoted unilateral addition of Grignard reagents to β-diketones: one-pot syntheses of β-tertiary hydroxyl ketones or 3-substituted cyclic-2-enones. *Org. Biomol. Chem.* **2016**, *14*, 724−728.

(6) (a) Hall, D. G. *Boronic Acids: Preparation, Applications in Organic Synthesis and Medicine*; John Wiley & Sons, 2006. (b) Candeias, N. R.; Montalbano, F.; Cal, P. M. S. D.; Gois, P. M. P. Boronic Acids and Esters in the Petasis-Borono Mannich Multicomponent Reaction. *Chem. Rev.* **2010**, *110*, 6169−6193. (c) Matteson, D. S.; Mah, R. W. H. Neighboring Boron in Nucleophilic Displacement. *J. Am. Chem. Soc.* **1963**, *85*, 2599−2603. (d) Petasis, N. A.; Zavialov, I. A. A New and Practical Synthesis of α-Amino Acids from Alkenyl Boronic Acids. *J. Am. Chem. Soc.* **1997**, *119*, 445−446. (e) Stymiest, J. L.; Dutheuil, G.; Mahmood, A.; Aggarwal, V. K. Lithiated carbamates: chiral carbenoids for iterative homologation of boranes and boronic esters. *Angew. Chem., Int. Ed.* **2007**, *46*, 7491−7494. (f) Barluenga, J.; Tomas-Gamasa, M.; Aznar, F.; Valdes, C. Metal-free carbon-carbon bond-forming reductive coupling between boronic acids and tosylhydrazones. *Nat. Chem.* **2009**, *1*, 494−499. (g) Zhang, L.; Lovinger, G. J.; Edelstein, E. K.; Szymaniak, A. A.; Chierchia, M. P.; Morken, J. P. Catalytic conjunctive cross-coupling enabled by metal-induced metallate rearrangement. *Science* **2016**, *351*, 70−74. (h) Kischkewitz, M.; Okamoto, K.; Mück-Lichtenfeld, C.; Studer, A. Radical-polar crossover reactions of vinylboron ate complexes. *Science* **2017**, *355*, 936−938. (i) Wang, H.; Jing, C.; Noble, A.; Aggarwal, V. K. Stereospecific 1,2-Migrations of Boronate Complexes Induced by Electrophiles. *Angew. Chem., Int. Ed.* **2020**, *59*, 16859−16872. (j) Sharma, H. A.; Essman, J. Z.; Jacobsen, E. N. Enantioselective catalytic 1,2-boronate rearrangements. *Science* **2021**, *374*, 752−757. (k) Xie, Q.; Dong, G. Aza-Matteson Reactions via Controlled Mono- and Double-Methylene Insertions into Nitrogen-Boron Bonds. *J. Am. Chem. Soc.* **2021**, *143*, 14422−14427. (l) Yang, Y.; Tsien, J.; Hughes, J. M. E.; Peters, B. K.; Merchant, R. R.; Qin, T. An intramolecular coupling approach to alkyl bioisosteres for the synthesis of multisubstituted bicycloalkyl boronates. *Nat. Chem.* **2021**, *13*, 950−955. (m) Wang, D.; Mück-Lichtenfeld, C.; Daniliuc, C. G.; Studer, A. Radical Aryl Migration from Boron to Carbon. *J. Am. Chem. Soc.* **2021**, *143*, 9320−9326. (n) Li, X.; Chen, H.; Wang, H.; Zhang, Q.; Sheng, H.; Lan, Y.; Song, Q. Transition-metal-free C(sp2)−C(sp3) cross-coupling of α-(pseudo)halo aliphatic ketones with boronic acids via a 1,4-metallate shift. *Nat. Synth.* **2023**, *2*, 1211−1221. (o) Ma, X.; Li, L.; Tan, M.; Zhong, Z.; Liang, J.; Li, P.; Song, Q. Modular assembly of versatile tetrasubstituted alkenyl monohalides from alkynyl tetracoordinate borons. *Chem* **2023**, *9*, 1164−1181. (p) Michel, M.; Weber, M.; Jayaraman, A.; Dewhurst, R. D.; Krummenacher, I.; Voigt, C.; Härterich, M.; Vargas, A.; Braunschweig, H. Olefin π-coordination chemistry at low-oxidation-state boron. *Nat. Chem.* **2026**, *18*, 135−141.

(7) (a) Hao, K.; Li, D.; Fu, D.; Zou, P.; Xie, S.; Lan, Y.; Chen, Y. Metal-Free 1,3-Boronate Rearrangement to Ketones Driven by Visible Light. *Angew. Chem., Int. Ed.* **2024**, *63*, No. e202316481. (b) Zou, P.; Fu, D. M.; Wang, H. Y.; Sun, R. Y.; Lan, Y.; Chen, Y. Y.

Downloaded from pubs.acs.org/jacsau/article-pdf/6/8/4458/6626357/jacsau.6c00455.pdf by SHANGHAI INST OF ORGANIC CHEMISTRY, Yiyun Chen on 07 September 2026

Photochemical 1,3-boronate rearrangement enables three-component N-alkylation for α-tertiary hydroxybenzylamine synthesis. *Nat. Commun.* **2024**, *15*, 10234.
(8) Smith, M. B.; March, J. Addition to Carbon−Hetero Multiple Bonds.. *March's Advanced Organic Chemistry*; John Wiley & Sons, 2006; pp. 1251−1476.
(9) (a) Mandal, D. K. Chapter 8 - Sigmatropic Rearrangements 1: [1,j] Shifts. In *Pericyclic Chemistry*; Elsevier, 2018; pp. 343−369. (b) Sedgwick, A. C.; Wu, L.; Han, H.-H.; Bull, S. D.; He, X.-P.; James, T. D.; Sessler, J. L.; Tang, B. Z.; Tian, H.; Yoon, J. Excited-state intramolecular proton-transfer (ESIPT) based fluorescence sensors and imaging agents. *Chem. Soc. Rev.* **2018**, *47*, 8842−8880. (c) Goodman, J.; Brus, L. E. Proton transfer and tautomerism in an excited state of methyl salicylate. *J. Am. Chem. Soc.* **1978**, *100*, 7472−7474. (d) Ansorg, K.; Braunschweig, H.; Chiu, C. W.; Engels, B.; Gamon, D.; Hugel, M.; Kupfer, T.; Radacki, K. The pentaphenylborole-2,6-lutidine adduct: a system with unusual thermochromic and photochromic properties. *Angew. Chem., Int. Ed.* **2011**, *50*, 2833−2836.
(10) TA experiments support ESIPT as a competitive pathway.
(11) Replacing the heterocycle with other functional groups (such as phenyl, ester, or amide) resulted in significantly lower yields, highlighting that the heteroaromatic nitrogen is essential for ESIPT suppression and the subsequent 1,5-sigmatropic migration (Figure S7).
(12) Chikashita, H.; Ishibaba, M.; Ori, K.; Itoh, K. General Reactivity of 2-Lithiobenzothiazole to Various Electrophiles and the Use as a Formyl Anion Equivalent in the Synthesis of α-Hydroxy Carbonyl Compounds. *Bull. Chem. Soc. Jpn.* **1988**, *61*, 3637−3648.
(13) (a) Eastgate, M. D.; Schmidt, M. A.; Fandrick, K. R. On the design of complex drug candidate syntheses in the pharmaceutical industry. *Nat. Rev. Chem.* **2017**, *1*, 0016. (b) Blakemore, D. C.; Castro, L.; Churcher, I.; Rees, D. C.; Thomas, A. W.; Wilson, D. M.; Wood, A. Organic synthesis provides opportunities to transform drug discovery. *Nat. Chem.* **2018**, *10*, 383−394.
(14) Xu, C. Y.; Zhang, Y. X.; Chen, Y. Y. Photochemical Boronate Rearrangement Enables the One-Pot Synthesis of 2,4-Difunctionalized 2-Chromenes. *Org. Lett.* **2026**, *28*, 3997−4002.
(15) Bandgar, B. P.; Sarangdhar, R. J.; Khan, F.; Mookkan, J.; Shetty, P.; Singh, G. Synthesis and Biological Evaluation of Orally Active Hypolipidemic Agents. *J. Med. Chem.* **2011**, *54*, 5915−5926.
(16) Cernak, T.; Dykstra, K. D.; Tyagarajan, S.; Vachal, P.; Krska, S. W. The medicinal chemist's toolbox for late stage functionalization of drug-like molecules. *Chem. Soc. Rev.* **2016**, *45*, 546−576.
(17) (a) Pillitteri, S.; Ranjan, P.; Van der Eycken, E. V.; Sharma, U. K. Uncovering the Potential of Boronic Acid and Derivatives as Radical Source in Photo(electro)chemical Reactions. *Adv. Synth. Catal* **2022**, *364*, 1643−1665. (b) Marotta, A.; Adams, C. E.; Molloy, J. J. The Impact of Boron Hybridisation on Photocatalytic Processes. *Angew. Chem., Int. Ed.* **2022**, *61*, No. e202207067. (c) Yasu, Y.; Koike, T.; Akita, M. Visible Light-Induced Selective Generation of Radicals from Organoborates by Photoredox Catalysis. *Adv. Synth. Catal* **2012**, *354*, 3414−3420. (d) Tellis, J. C.; Primer, D. N.; Molander, G. A. Single-electron transmetalation in organoboron cross-coupling by photoredox/nickel dual catalysis. *Science* **2014**, *345*, 433−436. (e) Huang, H.; Zhang, G.; Gong, L.; Zhang, S.; Chen, Y. Visible-light-induced chemoselective deboronative alkynylation under biomolecule-compatible conditions. *J. Am. Chem. Soc.* **2014**, *136*, 2280−2283. (f) Lima, F.; Kabeshov, M. A.; Tran, D. N.; Battilocchio, C.; Sedelmeier, J.; Sedelmeier, G.; Schenkel, B.; Ley, S. V. Visible Light Activation of Boronic Esters Enables Efficient Photoredox $C(sp^2)$-$C(sp^3)$ Cross-Couplings in Flow. *Angew. Chem., Int. Ed.* **2016**, *55*, 14085−14089.
(18) (a) Vogler, T.; Studer, A. Applications of TEMPO in synthesis. *Synthesis* **2008**, *2008*, 1979−1993. (b) Clark, K. F.; Tyerman, S.; Evans, L.; Robertson, C. M.; Nelson, D. J.; Kennedy, A. R.; Murphy, J. A. A Hierarchy of Ligands Controls Formation and Reaction of Aryl Radicals in Pd-Catalyzed Ground-State Base-Promoted Coupling Reactions. *J. Am. Chem. Soc.* **2023**, *145*, 20849−20858.
(19) (a) Griller, D.; Ingold, K. U. Free-radical clocks. *Acc. Chem. Res.* **1980**, *13*, 317−323. (b) Xie, S.; Li, D.; Huang, H.; Zhang, F.; Chen, Y. Intermolecular Radical Addition to Ketoacids Enabled by Boron Activation. *J. Am. Chem. Soc.* **2019**, *141*, 16237−16242. (c) Cai, R.; Zou, P.; Zhang, Y.; Chen, Y. Chemoselective Synthesis of alpha-Tertiary Hydroxy Oximes via Photochemical 1,3-Boronate Rearrangement. *Org. Lett.* **2024**, *26*, 7795−7799.
(20) The decreased e.r. value may be due to the racemization of benzyl trifluoborates under the light irradiation.
(21) Csákÿ, A. G.; Herrán, G. D. L.; Murcia, M. C. Conjugate addition reactions of carbon nucleophiles to electron-deficient dienes. *Chem. Soc. Rev.* **2010**, *39*, 4080−4102.
(22) Höpfl, H. The tetrahedral character of the boron atom newly defined—a useful tool to evaluate the N→B bond. *J. Organomet. Chem.* **1999**, *581*, 129−149.
(23) Martinez-Aguirre, M. A.; Flores Alamo, M.; Elisa Trejo-Huizar, K.; Yatsimirsky, A. K. Boronic acid complexes with amino phenolic N,O-ligands and their use for non-covalent protein fluorescence labeling. *Bioorg. Chem.* **2021**, *113*, 104993.
(24) (a) Bull, S. D.; Davidson, M. G.; van den Elsen, J. M. H.; Fossey, J. S.; Jenkins, A. T. A.; Jiang, Y.-B.; Kubo, Y.; Marken, F.; Sakurai, K.; Zhao, J.; et al. Exploiting the Reversible Covalent Bonding of Boronic Acids: Recognition, Sensing, and Assembly. *Acc. Chem. Res.* **2013**, *46*, 312−326. (b) Malapit, C. A.; Bour, J. R.; Brigham, C. E.; Sanford, M. S. Base-free nickel-catalysed decarbonylative Suzuki−Miyaura coupling of acid fluorides. *Nature* **2018**, *563*, 100−104.
(25) Markov, P. Light-induced tautomerism of β-dicarbonyl compounds. *Chem. Soc. Rev.* **1984**, *13*, 69−96.
(26) Chen, C.-L.; Chen, Y.-T.; Demchenko, A. P.; Chou, P.-T. Amino proton donors in excited-state intramolecular proton-transfer reactions. *Nat. Rev. Chem.* **2018**, *2*, 131−143.
(27) Nano, A.; Gullo, M. P.; Ventura, B.; Armaroli, N.; Barbieri, A.; Ziessel, R. Panchromatic luminescence from julolidine dyes exhibiting excited state intramolecular proton transfer. *Chem. Commun.* **2015**, *51*, 3351−3354.
(28) Zhao, Y.; Truhlar, D. G. The M06 suite of density functionals for main group thermochemistry, thermochemical kinetics, noncovalent interactions, excited states, and transition elements: two new functionals and systematic testing of four M06-class functionals and 12 other functionals. *Theor. Chem. Acc.* **2008**, *120*, 215−241.
(29) Mantina, M.; Chamberlin, A. C.; Valero, R.; Cramer, C. J.; Truhlar, D. G. Consistent van der Waals Radii for the Whole Main Group. *J. Phys. Chem. A* **2009**, *113*, 5806−5812.
(30) van Stokkum, I. H. M.; Larsen, D. S.; van Grondelle, R. Global and target analysis of time-resolved spectra. *Biochim. Biophys. Acta, Bioenerg.* **2004**, *1657*, 82−104.
(31) Kandappa, S. K.; Valloli, L. K.; Ahuja, S.; Parthiban, J.; Sivaguru, J. Taming the excited state reactivity of imines − from non-radiative decay to aza Paternò−Büchi reaction. *Chem. Soc. Rev.* **2021**, *50*, 1617−1641.

Downloaded from pubs.acs.org/jacsau/article-pdf/6/8/4458/6626385/jacsau.6c00455.pdf by SHANGHAI INST OF ORGANIC CHEMISTRY, Yiyun Chen on 07 September 2026

https://doi.org/10.1021/jacsau.6c00455
JACS Au 2026, 6, 4458−4468